Effects of Xe postbombardment on carbonitrides produced in a lowcarbon nitrogen implanted steel

M. Behar, L. Amaral, S. M. M. Ramos, A. Vasquez, and F. C. Zawislak

Citation: Journal of Applied Physics **68**, 4487 (1990); doi: 10.1063/1.346199
View online: http://dx.doi.org/10.1063/1.346199
View Table of Contents: http://scitation.aip.org/content/aip/journal/jap/68/9?ver=pdfcov
Published by the AIP Publishing

Effects of Xe post-bombardment on carbonitrides produced in a low-carbon nitrogen-implanted steel

M. Behar, L. Amaral, S. M. M. Ramos, A. Vasquez, and F. C. Zawislak
Instituto de Física, UFRGS, 91500 Porto Alegre, RS, Brasil

(Received 13 February 1990; accepted for publication 22 June 1990)

The effects of Xe bombardment on carbonitrides produced by N implantation in a low-carbon steel are studied via conversion electron Mössbauer spectroscopy and nuclear reaction analysis. The results show two main features: dissolution and reprecipitation of the produced carbonitrides and modification of the thermal behavior of the precipitates. Recently we have performed similar experiments bombarding samples of the same steel with He and Ar. Comparison of the experiments shows that irradiation with Ar ions provides the best retention of carbonitrides at 450 °C. On the other hand, irradiation with Xe ions to the same dpa level is most effective in producing the dissolution and reprecipitation process.

I. INTRODUCTION

Nitrogen implantation is presently a well-known process commonly used by many laboratories and industries in order to improve the tribological properties of steels.[1,2] On the other hand the effects caused by ion bombardment on nitrides and carbonitrides (produced by ion implantation) is a subject that has received much less attention. During the last four years we have performed a systematic study of the effects produced by alpha and by Ar bombardment of nitrides and carbonitrides precipitates produced in Fe,[3] in low carbon[4,5] and in carbon-Cr[6] steels. Two important features have emerged from our work: (a) The ion implantation affects the thermal behavior of the carbonitrides present in the sample, raising their dissolution temperature; (b) ion irradiation produces, in most cases, dissolution and reprecipitation of the carbonitrides. Despite these common general features, each of the systems studied also has shown its own peculiar characteristics. In fact, the amount of retained carbonitrides strongly depends on the type of ion used for irradiation. However, the highest temperature at which the precipitates are still retained seems to be only a function of the composition of the implanted matrix. On the other hand, the dissolution and reprecipitation processes are strongly related to the type of ion used, the kind of carbonitride phase being irradiated, and the composition of the matrix in which the precipitates have been formed.

Our previous works have left several open questions. It is not clear if the mass of the bombarding ion is the only relevant parameter in the retention of the carbonitrides during high temperature aging. It seems that the damage created by the implantation process is not the unique feature influencing the dissolution and reprecipitation process. For the same displacement-per-atom (dpa) fluence, we have obtained quite different results using He or Ar as the bombarding ion. Moreover, it appears that the matrix composition also plays an important role in this last phenomenon.

In order to answer some of the above questions, we have undertaken the present work. Here, we report results of Xe irradiation of carbonitrides produced by N implantation in a low-carbon steel. The precipitates formed during Xe ion irradiation have then been subjected to various thermal treatments. The characterization and evolution of the precipitates have been followed in each stage using ^{57}Fe conversion electron spectroscopy (CEMS). In addition the nitrogen depth profiles for implanted and annealed sample were measured using the Nuclear Reaction Analysis (NRA) technique.

II. EXPERIMENTAL PROCEDURE

Samples obtained from industrial ingots of 1020 low-carbon steel (0.2 C: 0.9 Mn, wt %) were mechanically polished and then implanted at the ion implantor of the Institute of Physics, Porto Alegre. The N_2^+ ions have been implanted at 140, 80, and 40 keV in order to obtain a plateau in the ion distribution with depth from near the surface up to approximately 2000 Å. Typical fluences were 6×10^{16} N_2/cm^2 and the N concentration at the plateau was around 40 at. %. The Xe irradiation was done using an ion energy of 500 keV corresponding to a projected range of 652 Å,[7] therefore leaving the Xe particles in the N-implanted region. The samples were studied as a function of the Xe fluence in the 10^{14}–10^{16} Xe/cm^2 range. The current density during the N and Xe implantations was always less than 1 $\mu A/cm^2$ in order to avoid heating of the samples. In addition during the implantation process the sample was cooled in order to be kept at 20 °C.

Two types of N_2^+ implanted samples were studied. One type which was first Xe irradiated and then annealed at 400 °C, will be referred to as the [1020 N (Xe, 400)] sample. The other type, which was first annealed at 400 °C and then irradiated with Xe, will be referred to as the [1020 N (400, Xe)] sample. These and further anneals at 450 °C and 500 °C were performed in a vacuum of better than 10^{-6} Torr for 1 h each. All the Xe irradiations were performed at room temperature.

The CEMS data were obtained in a backscattering geometry. A proportional counter in which He-5% CH_4 was allowed to flow was added to a conventional constant acceleration Mössbauer spectrometer. The 7.3 keV K-conversion and 5.6 keV Auger electrons are excited by the 14.4 keV γ radiation from a ^{57}Co radioactive source in a Rh matrix. In addition, the N depth distributions were profiled through the $^{14}N(p,\gamma)^{15}O$ reaction[8] in the as-implanted condition

 0021-8979/90/214487-07$03.00

TABLE I. ^{57}Fe Mössbauer parameters obtained from the least square fit to the present data. H_1, H_2, H_3, and H_4 are the sets of characteristic magnetic fields corresponding to Fe, ϵ-Fe$_{2+x}$(C,N), ϵ-Fe$_{3,2}$(C,N), and θ-Fe$_3$(C,N), respectively and Q_1 and Q_2 are the characteristic quadrupole splitting corresponding to ϵ-Fe$_2$(C,N) and ϵ-Fe$_{2+x}$(C,N). The isomer shift δ is given relative to Fe metal at room temperature.

	H (kG)		E_{eQ} (mm/s)	δ (mm/s)
Fe	331 ± 3	H_1		0.01 ± 0.02
ϵ-Fe$_{2+x}$(C,N)	279 ± 4			0.27 ± 0.05
	218 ± 4	H_2		0.25 ± 0.02
	133 ± 5		− 0.06 ± 0.02	0.43 ± 0.04
		Q_2	0.76 ± 0.02	
ϵ-Fe$_{3,2}$(C,N)	238 ± 3	H_3		0.31 ± 0.02
	298 ± 3			0.24 ± 0.04
θ-Fe$_3$(C,N)	198 ± 5	H_4		0.45 ± 0.02
ϵ-Fe$_2$(C,N)		Q_1	0.32 ± 0.02	0.40 ± 0.02

and after post-irradiation annealing. The γ-rays were detected using a 3′×3′ NaI(Tl) scintillator detector.

III. RESULTS

Well-characterized nitrides and carbonitrides formed by standard techniques in different kinds of steels have been extensively investigated via Mössbauer spectroscopy. As a consequence their characteristic hyperfine parameters (internal magnetic field H, isomer shift δ, and quadrupole splitting ΔE_Q) are nowadays well established. Table I shows the parameters used in the present work which agree with those published previously.[2] Tables II and III display the normalized CEMS spectrum areas for the martensitic phase and the carbonitride precipitates present in each sample at various stages of the experiment.

A. 1020 N (Xe, 400) sample

The CEMS spectrum of the N_2^+ implanted sample is shown in Fig. 1(a). In addition to the characteristic sextet of the martensitic phase, the spectrum also displays a quadrupole doublet typical of ξ or ϵ-Fe$_2$(C,N), plus a minor contribution from θ-Fe$_3$(C,N). As is well discussed in the literature[9] it is not possible to distinguish, only via Mössbauer measurements, between ϵ and ξ nitrides or carbonitrides. However, results from small-angle x ray diffraction experiments performed on similar systems[2] have shown that carbonitrides are always formed whenever a carbon steel is N implanted. Moreover, it was argued in Refs. 9 and 10 that this situation occurs whenever a N implantation is performed on a carbon steel. Therefore, in what follows we assume that our sample contains carbonitrides, rather than nitrides in particular ϵ-Fe$_2$(C,N) precipitates.

The Xe irradiation to a fluence of 2.5×10^{15} atoms/cm^2 considerably changes the CEMS spectrum, as shown in Fig. 1(b). The new spectrum shows a drastic dissolution of the ϵ-Fe$_2$(C,N) and a formation of ϵ-Fe$_{2+x}$(C,N) carbonitride[2] (with $x<1$). Table II shows that the amount of ϵ-Fe$_2$(C,N) was reduced from 48% to only 8%. Dissolution feature is also observed for the θ-Fe$_3$(C,N) precipitate which after the Xe irradiation is reduced to about 50% of its original amount.

The subsequent annealing of the sample at 400 °C produces a complete dissolution of the ϵ-Fe$_2$(C,N) and ϵ-Fe$_{2+x}$(C,N) compounds and a formation of a ϵ-Fe$_{3,2}$(C,N) carbonitrides—see Fig. 1(c). At this stage, a significant part of the total CEMS area (55%) still corresponds to carbonitrides. However, annealing at 450 °C drastically reduces the precipitate concentration to only 5%—as

TABLE II. Normalized CEMS spectral areas (in %) of carbonitride precipitates for [1020 N (Xe,400)] sample irradiated at 2.5×10^{15} Xe/cm^2 fluence. Typical errors are ± 5%.

Precipitates / Sample	Fe Matrix	ϵ-Fe$_2$(C,N)	ϵ-Fe$_{3,2}$(C,N)	ϵ-Fe$_{2+x}$(C,N)	θ-Fe$_3$(C,N)
1020 + N	0.35	0.48	···	···	0.17
Xe(2.5×10^{15})	0.40	0.08	···	0.40	0.12
400 °C	0.45	···	0.46	···	0.09
450 °C	0.95	···	0.05	···	···
500 °C	1.00	···	···	···	···

TABLE III. Normalized CEMS spectral areas of carbonitride precipitates annealed and irradiated with different Xe fluences. The six samples have been initially equally N implanted and annealed at 400 °C [1020 N (400,Xe)] samples. Typical errors are ± 5%.

Sample	Fe Matrix	Precipitates ϵ-$Fe_2(C,N)$	ϵ-$Fe_{3.2}(C,N)$	ϵ-$Fe_{2+x}(C,N)$	θ-$Fe_3(C,N)$
1020 + N	0.35	0.48	···	···	0.17
400 °C	0.53	···	0.36	···	0.11
Sample 1					
Xe(10^{14})	0.54	···	···	0.38	0.08
450°C	1.00	···	···	···	···
Sample 2					
Xe(8×10^{14})	0.55	···	···	0.36	0.09
450 °C	0.97	···	0.03	···	···
Sample 3					
Xe(10^{15})	0.45	···	···	0.42	0.13
450 °C	0.94	···	0.06	···	···
Sample 4					
Xe(2.5×10^{15})	0.37	···	···	0.46	0.17
450 °C	0.61	···	0.35	···	0.04
Sample 5					
Xe(5×10^{15})	0.42	···	···	0.43	0.15
450 °C	0.87	···	0.13	···	···
Sample 6					
Xe(10^{16})	0.43	···	···	0.43	0.14
450 °C	0.92	···	0.08	···	···

shown in Fig. 1(d). Finally annealing at 500 °C dissolves all the carbonitrides present in the analyzed region.

B. [1020 N_2^+ (400, Xe)] sample

The 400 °C anneal of the N_2^+ implanted sample produces: a complete dissolution of the ϵ-$Fe_2(C,N)$, a partial one of the θ-$Fe_3(C,N)$ carbonitride and a formation of ϵ-$Fe_{3.2}(C,N)$ precipitates—see Fig. 2(a) and Table III.

Irradiation of the above specimen with Xe ions to a dose of 2.5×10^{15} at/cm^2 (sample 4) changes completely the CEMS spectrum as shown in Fig. 2(b) and described by Table III. The ϵ-$Fe_{3.2}(C,N)$ precipitate has been completely dissolved and reprecipitated into ϵ-$Fe_{2+x}(C,N)$ $(x<1)$. On the other hand, the θ-$Fe_3(C,N)$ carbonitrides remains stable. The data of Table III shows that variation in the Xe bombarding fluence between $\phi = 10^{14}$ Xe/cm^2 and 10^{16} Xe/cm^2 does not produce any further effect on the reprecipitation process.

The subsequent 450 °C annealing of sample 4 produces a complete dissolution of the ϵ-$Fe_{2+x}(C,N)$ carbonitrides and reformation of the ϵ-$Fe_{3.2}(C,N)$ phase, as is shown in Fig. 2(c) and Table III. At this stage the CEMS spectrum shows that there is a considerable amount of carbonitrides present. Further annealing at 500 °C completely dissolves all precipitates.

An inspection of Table III shows that the retention of the carbonitrides at 450 °C strongly depends on the previous Xe-implanted fluence. In fact, for the lowest fluence (sample 1) there is no retention at all. With increasing fluence the amount of retained carbonitrides increases (samples 2 and 3). A maximum is reached at 0.5 at. % (sample 4) and then for the remaining Xe fluences (samples 5 and 6) there is a continuous decrease in the amount of retained precipitates.

The nitrogen evolution during different stages of the experiment was followed by the N.R.A. technique. The as-implanted profile of the N implanted sample (1020 + N) is shown in Fig. 3. The ion distribution goes from near the surface up to around 2000 Å and the plateau concentration is around 40%. A subsequent anneal performed at 450 °C produces a nitrogen diffusion from the plateau region and consequently drastically reduces the particle concentration to

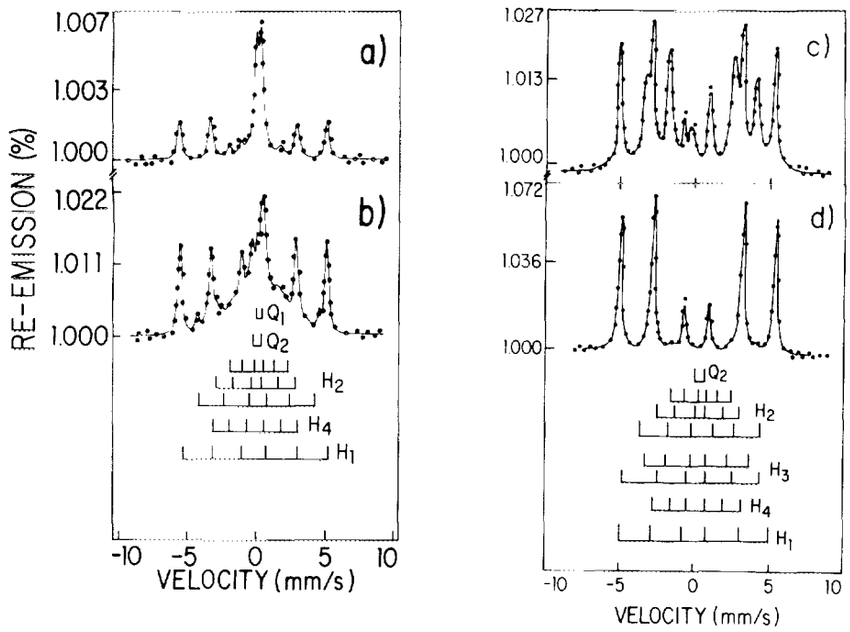

FIG. 1. ^{57} CEMS spectra measured at room temperature for 1020 steel (a) implanted with N_2^+, (b) same as (a) after Xe post-bombardment with $\phi = 2.5\times10^{15}$ Xe/cm^2, (c) same as (b) after annealing at 400 °C for 1 h, (d) same as (c) after annealing at 450 °C for 1 h.

less than 10%—[(1020 + N) + 450 °C] profile. Instead, similar annealing of a previously Xe-irradiated sample [(1020 + N) + Xe + 450 °C] produces a much smaller reduction in the N concentration, as can be observed from the figure. This behavior certainly should be attributed to the presence of Xe in the N-implanted region.

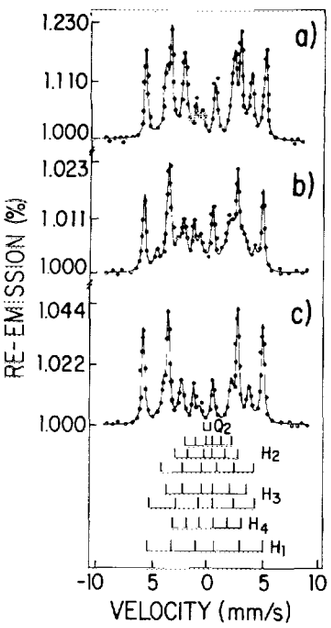

FIG. 2. ^{57}Fe spectra measured at room temperature for 1020 steel a) N_2^+ implanted and annealed at 400 °C for 1 h. b) same as (a) and irradiated with $\phi = 2.5\times10^{15}$ Xe/cm^2, c) same as (b) after annealing at 450 °C for 1 h.

IV. DISCUSSION

The Xe irradiation of the carbonitrides formed by N implantation in the 1020 carbon steel produces two main features: (i) dissolution and then reprecipitation of the carbonitrides; (ii) modification of the thermal behavior of the precipitates. These features are going to be discussed separately.

A. Dissolution and reprecipitation

Table II shows that for $\phi = 2.5\times10^{15}$ Xe/cm^2 (which corresponds to 50 dpa) there is drastic dissolution of the

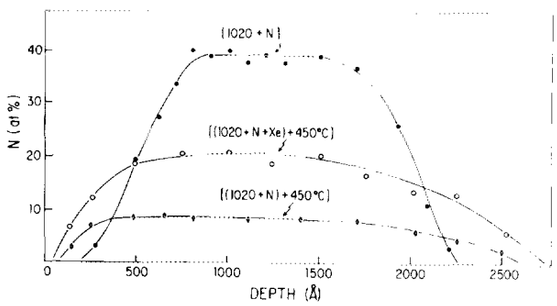

FIG. 3. Nitrogen profiles obtained through the NRA technique. [1020 + N]: as implanted profile of the N implanted sample. [(1020 + N) + 450)]: same as before and annealed at 450 °C. [(1020 + N + Xe) + 450 °C]: profile of a nitrogen implanted sample, Xe post-bombarded and further annealed at 450 °C.

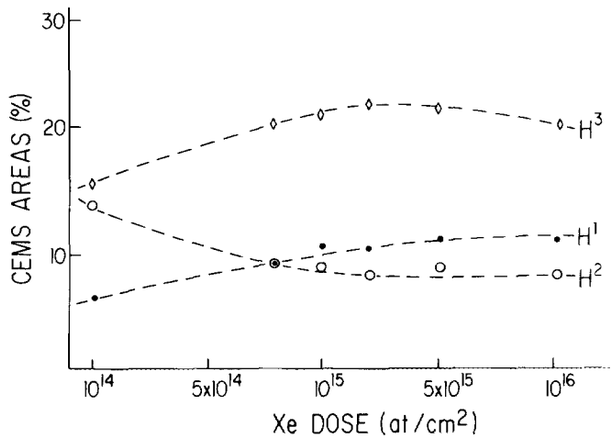

FIG. 4. Normalized CEMS subspectral areas corresponding to one (H^1), two (H^2), and three (H^3) near neighbors to iron atoms at different Xe fluence. The lines are drawn only to guide the eye.

ϵ-$Fe_2(C,N)$ carbonitrides and reprecipitation of the ϵ-$Fe_{2+x}(C,N)$ phase.

On the other hand, analyzing the Xe irradiation data of the ϵ-$Fe_{3.2}(C,N)$ carbonitrides, it is possible to observe that already for the lowest dose (corresponding to ~ 1 dpa) there is a complete ϵ-$Fe_{3.2} \rightarrow \epsilon$-$Fe_{2+x}(C,N)$ transformation. The ϵ-$Fe_{2+x}(C,N)$ carbonitrides have an hcp crystal structure where C and N are interstitial nearest neighbors (nn) to the iron atoms.[11] The magnetic hyperfine fields corresponding to one, two, and three nn are $H_2^1 = 279$ kG, $H_2^2 = 218$ kG, and $H_2^3 = 133$ kG, respectively.[2,11] Therefore, from the Mössbauer spectrum and the resonant areas of each subpattern, it is possible to determine the population that corresponds to each nn configuration. In Fig. 4, the evolution of the 1, 2, and 3 nn populations are shown for the ϵ-$Fe_{3.2}(C,N) \rightarrow \epsilon$-$Fe_{2+x}(C,N)$ transformation. The main features of this evolution are: the increase in the 1 nn population and the decrease in the 2 nn population with increasing Xe irradiation fluence. Therefore, one observes that the particle bombardment not only produces the ϵ-$Fe_{3.2}(C,N) \rightarrow \epsilon$-$Fe_{2+x}(C,N)$ transformation, but also changes the nn populations. This variation should in principle be reflected in the final stoichiometry of the ϵ-$Fe_{2+x}(C,N)$ precipitates. However, an inspection of Table IV shows that x is almost independent of the bombarding fluence, its value varying between 0.6 and 0.7.

It is interesting to compare the present data with the He[4] and Ar[5] post-bombardment irradiation results.

(a) The Xe irradiation is the most effective in dissolving the ϵ-$Fe_2(C,N)$ precipitates. For a Xe irradiation fluence of 20 dpa, 84% of the carbonitrides are dissolved. By contrast, Ar irradiation to 50 dpa dissolves only 50% of the ϵ-$Fe_2(C,N)$ precipitates.[5] Finally, an alpha irradiation of 1.5 dpa is not able to produce any noticeable carbonitride dissolution.[4]

(b) The ϵ-$Fe_{3.2}(C,N)$ carbonitrides are very unstable during particle irradiation. Xe, Ar, and He seems to be equally effective in dissolving these precipitates. However, the different bombarding ions produce different nn configurations in the resulting ϵ-$Fe_{2+x}(C,N)$ carbonitrides. For approximately the same 1 dpa fluence the He irradiation produces almost equal 1, 2, and 3 nn populations (around 15%).[4] For Ar, the 3 nn population is around 24% while the other two nn configurations are around 14%.[5] Finally, for Xe the 1 nn population is of 6% and the 2 and 3 nn population are around 15%.

(c) The final stoichiometry of the ϵ-$Fe_{2+x}(C,N)$ carbonitrides formed from the ϵ-$Fe_{3.2}(C,N) \rightarrow \epsilon$-$Fe_{2+x}(C,N)$ transformation seems to be a function of the bombarding ion, but not of the fluence. In Fig. 5 are displayed for each bombarding ion the final stoichiometry as a function of the dpa fluence (for the He case we quoted only the values near 1 dpa). An inspection of the figure reveals a correlation between the x values and the ion used during the bombardment. For He, x oscillates between 0.8 and 0.9, for Ar $0.7 \leqslant x \leqslant 0.8$ and for Xe $0.6 \leqslant x \leqslant 0.7$. Therefore, it seems that the heavier the bombarding ion is the richer the carbonitride phase. This is a tentative statement because the x values are affected by an uncertainty of 10%–15%. Nevertheless a systematic trend seem to emerge from the set of data taken as a whole.

Extensive work has been done in the last several years studying the stability of coherent and semicoherent precipitates under heavy ion and neutron irradiations—see for example reference 12. However, these studies have not lead to one unique explanation for the mechanisms of dissolution and reprecipitation of the precipitates. Nelson *et al.*[13] have argued that the dissolution and reprecipitation processes are due to competitive effects between radiation enhanced diffusion and cascade disordering and/or dissolution. On the other hand, Vaidja[14] claims that the stability of the precipitates under irradiation is due to interfacial dislocations. Loss or

TABLE IV. C or N interstitial near neighbor (nn) population for the Fe atoms in the ϵ-$Fe_{3.2}(C,N) \rightarrow \epsilon$-$Fe_{2+x}(C,N)$ transformation as function of Xe fluence. The bottom line represents the final ϵ-$Fe_{2+x}(C,N)$ stoichiometry after the Xe irradiation.

Xe fluence	10^{14} Xe/cm^2	8×10^{14} Xe/cm^2	10^{15} Xe/cm^2	2.5×10^{15} Xe/cm^2	5×10^{15} Xe/cm^2	10^{16} Xe/cm^2
1 nn	6	9	11	11	12	12
2 nn	14	9	9	8	9	8
3 nn	16	21	22	23	22	21
Fe_{2+x}	2.6	2.6	2.7	2.6	2.7	2.7

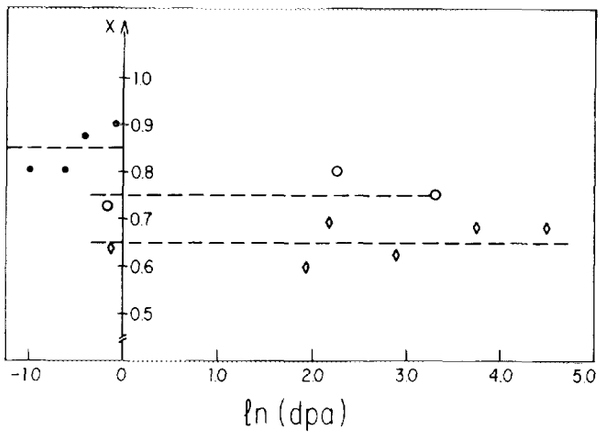

FIG. 5. X values as a function of the dpa fluence in the ϵ-$Fe_{3.2}(C,N) \rightarrow \epsilon$-$Fe_{2+x2}(C,N)$ transformation as a consequence of particle irradiation. Full points correspond to He bombardment. Open circles to Ar irradiation. Diamond to Xe bombardment. The lines are drawn only to guide the eye.

modifications of these dislocations would be responsible for the dissolution of the precipitates.

Our results can be explained, at lest qualitatively, by both models. They show that the dpa fluence is not the unique parameter that characterizes the dissolution of precipitates. Our results suggest that the cascade density produced during the bombardment also plays a major role (as predicted by both models). In fact, the larger the ion mass, the higher the cascade density produced by the ion bombardment. Thus, it is possible to understand why 1 dpa fluence of Ar ions is able to dissolve the ϵ-$Fe_2(C,N)$ while the He is not able to produce dissolution. Following the same arguments, it is not surprising to observe that Xe is the most efficient ion (for equal dpa fluence) in dissolving the ϵ-$Fe_2(C,N)$ carbonitride.

B. Thermal behavior of precipitates

Previous work[15,2] has shown that nitrides and carbonitrides produced in Fe and in carbon steels are stable only up to 400 °C. At higher temperatures, the precipitates dissolve as a consequence of N diffusing out from the implanted region.

The results of our NRA experiments clearly show that the presence of Xe atoms strongly inhibits the N diffusion. As a consequence, one should expect that the carbonitrides in Xe irradiated samples will remain stable during annealing at higher temperatures. This feature is fully confirmed by the CEMS experiments which show that the precipitates remain stable up to 450 °C.

All of these facts can be understood if we analyze the behavior of Xe in metals. In principle Xe is not soluble, but it can accumulate in large quantities via the formation of Xe-vacancy complexes (Xe-V). For low implantation fluences and at room temperature, small Xe-V systems are formed. However, for higher temperatures or for increasing Xe

TABLE V. Comparison of ϵ-$Fe_{3.2}(C,N)$ retentions after annealing at 450 °C for similar samples and post-bombarded at the same peak concentration with He, Ar, and Xe ions.

Ion	Sample	Retained ϵ-$Fe_{3.2}(C,N)$ at 450 °C (%)
He	1020 N(α,400)	5
He	1020 N(400,α)	20
Ar	1020 N(Ar,400)	15
Ar	1020 N(400,Ar)	44
Xe	1020 N(Xe,400)	5
Xe	1020 N(400,Xe)	35

fluences, the Xe-V complexes migrate and agglomerate and eventually form Xe bubbles. The above mechanism can be associated with the carbonitride retention effect observed in the present experiment. The implanted Xe creates Xe-V complexes which migrate to sinks, like grain boundaries, precipitates and dislocations. When the anneal is performed, two competitive processes can occur. First the Xe-V will act as trapping centers for the N atoms released from the precipitates. Therefore, the N diffusion would be inhibited and the precipitates will remain stable up to higher temperatures. Second the same annealing process will favor coarsening of the distribution of Xe-V complexes, making them larger and less concentrated, and therefore less efficient at inhibiting the N-diffusion mechanism.

The retention effect after annealing at 450 °C has been basically observed for the [1020 N (400 Xe)] sample. For the [1020 N (Xe,400)] specimen, retention is less efficient. As discussed in a previous paper,[4,5] the difference in the thermal behavior of both samples should not be attributed to the crystalline structure of the different precipitates involved in the thermal processes, ϵ-$Fe_{2+x2}(C,N)$ for the [1020 N (400,Xe)] and ϵ-$Fe_{3.2}(C,N)$ for the {1020 N (Xe,400)] one. Rather it should be related to thermal behavior of the Xe-V complexes. Analyzing the thermal behavior of both samples one observes that in the [1020 N (400,Xe)] case, the Xe-V complexes are submitted to only one annealing process performed at 450 °C. Instead for the other sample they are submitted to two successive annealings at 400 and 450 °C. Then the complexes should agglomerate more than in the first case becoming less efficient in retarding the N diffusion.

In Table V we compare for the same peak concentration (0.5 at. %) the previous He and Ar irradiation results with the present ones. In all the cases the Ar irradiation produces the highest amount of carbonitride retention. For the [1020 N (NG,400)] kind of sample (NG stands for He, Ar, or Xe) the Ar retention is three times higher than He or Xe (15% compared to 5%). On the other hand, for the [1020 N (400 NG)] samples the Ar produces a retention of 44%, the Xe 35% and the He only 20%.

Two more features should be pointed out. First, for all three ions the maximum retention occurs at the approximately same peak concentration (0.5 at. %). Second, the Ar retention effect is not only the most effective, but it also extends over the widest concentration range (see Fig. 6). In fact, for He, the retention starts at 0.35 at. % and ceases to be

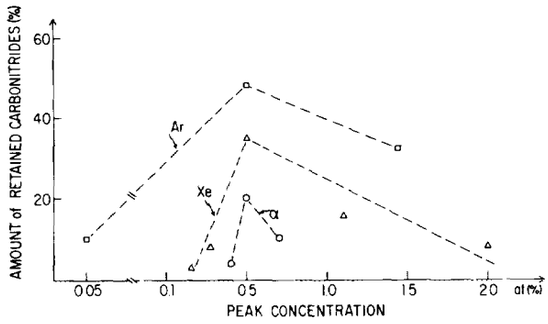

FIG. 6. Relative amount of carbonitrides retained after annealing at 450 °C as function of He, Ar, or Xe post-bombardment dose (measured in at. % at the peak).

effective at 0.75 at. %. The Xe starts to be effective at 0.15 at. % and still produces retention effect at 2 at. %. For Ar, the lowest concentration limit is 0.05 at. %, and it does not decreases significantly even at 1.4 at. %.

V. CONCLUSIONS

The present work shows that the carbonitrides produced in N-implanted 1020 carbon steel are affected by the Xe irradiation in two ways. First they are partially or totally dissolved by the post-bombardment. Second the presence of Xe ions in the N implanted region modifies the thermal behavior of the carbonitrides by raising the temperature of dissolution.

Comparison of the Xe, Ar, and He experiments show several interesting features. (a) For the same dpa fluence Xe irradiation most efficiently dissolves the ϵ-$Fe_2(C,N)$ precipitates. This result indicates that the cascade density plays an important role in the mechanism of dissolution. (b) For reprecipitation of ϵ-$Fe_{3.2}(C,N) \rightarrow \epsilon$-$Fe_{2+x}(C,N)$, all the bombarding ions are equally efficient. However, each implanted ion produces different nn configurations in the final carbonitride. Moreover, the ϵ-$Fe_{2+x}(C,N)$ stoichiometry appears to be affected by the type of ion used in the irradiation. For the heavier ion (Xe), the richest carbonitride is produced while for the lightest (He), the precipitate phase formed is the poorest in C and N of those possible. (c) In all cases, the noble gas irradiation modifies the subsequent thermal aging behavior of the carbonitrides. The maximum retention of precipitates occurs at the same atomic concentration of irradiating gas ions ($c = 0.5$ at. %). However, the Ar ion is not only the most efficient but also is most effective at the lowest atomic concentrations. These features suggest that the mass or the size of the bombarding ions are not the only relevant parameters in the retention effect.

The retention temperature is independent of the bombarding ion. On the other hand this temperature was higher when nitrides formed in Fe were bombarded with He.[3] Therefore, it should be concluded that the retention temperature is strongly related to the composition of the matrix.

[1]G. Longworth and E. W. Hartley, Thin Solid Films **48**, 95 (1978).
[2]G. Marest, in *Ion Implantation 1988*, edited by F. H. Wohlbier (Trans-Tech. Publication 1988) and references therein.
[3]M. Behar, P. J. Viccaro, M. T. X. Silva, A. Vasquez, C. A. dos Santos, and F. C. Zawislak, Nucl. Instrum. Methods B **19/20**, 132 (1987).
[4]S. M. M. Ramos, L. Amaral, M. Behar, G. Marest, A. Vasquez, and F. C. Zawislak, J. Phys. Condens. Matter **1**, 8799 (1989).
[5]S. M. M. Ramos, L. Amaral, M. Behar, G. Marest, A. Vasquez, and F. C. Zawislak, Radiat. Eff. Def. Solids **110**, 355 (1989).
[6]S. M. M. Ramos, L. Amaral, M. Behar, G. Marest, A. Vasquez, and F. C. Zawislak, Hyperfine Interactions (to be published).
[7]J. P. Biersack and L. G. Haggemark, Nucl. Instrum. Methods **174**, 257 (1980).
[8]J. W. Mayer and E. Rimini, Eds., *Ion Beam Handbook for Material Analysis*, (Academic, New York, 1987).
[9]C. A. dos Santos, M. Behar, and I. J. R. Baumvol, J. Phys. D **17**, 969 (1984) and references therein.
[10]G. Principi, P. Matteazi, E. Ramos, and G. Longworth, J. Mat. Sci. **15**, 2665 (1980).
[11]N. de Cristoforo and R. Kaplow, Met. Trans. A **8**, A425 (1977).
[12]K. Farrel, P. J. Maziasz, E. H. Lee, and L. K. Mansur, Rad. Eff. **78**, 227 (1983).
[13]R. S. Nelson, J. A. Hudson, and D. Y. Mazey, J. Nucl. Mat. **44**, 318 (1972).
[14]W. N. Vaidya, J. Nucl. Mat. **83**, 223 (1979).
[15]C. A. dos Santos, B. A. S. de Barros, Jr., J. P. de Souza, and I. J. R. Baumvol, Appl. Phys. Lett. **41**, 237 (1982) and C. A. dos Santos, Ph.D. thesis (unpublished).